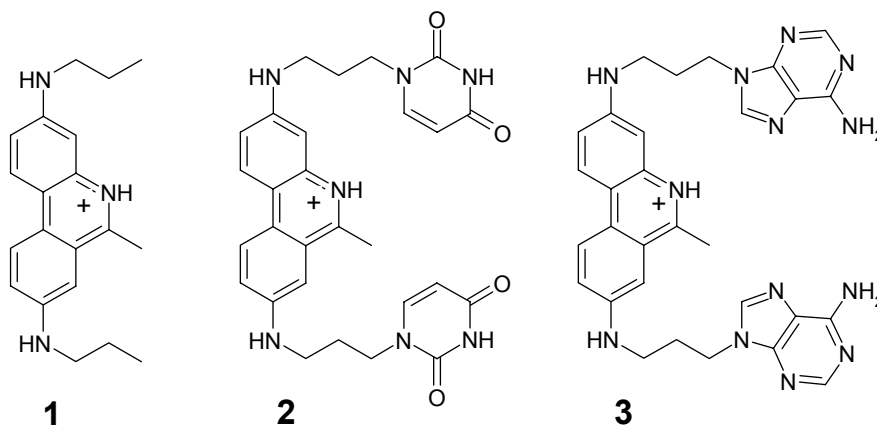


Recognition of homo-polynucleotides containing adenine by phenanthridinium bis-uracil conjugate in aqueous media.

^aLidija Tumir, ^aIvo Piantanida*, ^bIva Juranović, ^bZlatko Meić, ^cSanja Tomić, ^aMladen Žinić*

^a Laboratory of Supramolecular and Nucleoside Chemistry, Department of Chemistry and Biochemistry, Ruđer Bošković Institute, HR 10002 Zagreb, P.O.B. 180, Croatia; ^b Laboratory of Analytical Chemistry, Department of Chemistry, Faculty of Science, Strossmayerov trg 14, HR 10000 Zagreb, Croatia; ^c Laboratory for Chemical and Biological Crystallography, Department of Physical Chemistry, Ruđer Bošković Institute, HR 10002 Zagreb, P.O.B. 180, Croatia

All here presented compounds (**1-3**) were synthesized by modified procedures elaborated earlier for their close analogues¹, have satisfying elemental analyses and their structures were verified by detailed 1D and 2D NMR analysis, mass spectrometry and when possible elemental analysis. Hygroscopic character of **2** and **3** precipitates yielded elemental analyses with non-stoichiometric amounts of solvent – however, since NMR and mass spectra of these compounds are correct and they are obtained by simple chemical reactions from well characterized starting compounds their structures are not questionable. Detailed synthesis procedures and other experimental data will be published as a full paper elsewhere.



Scheme 1. Structures of novel phenanthridinium – bis-nucleobase conjugates.

Supplementary Material (ESI) for Chemical Communications
This journal is © The Royal Society of Chemistry 2005

3,8-Bis (propyl)amino-6-methylphenantridine (1) was obtained as a red powder in 67 % yield; mp 118-121 °C; ¹H-NMR (DMSO-d₆) δ: 0.98 (m, 2 × CH₃, 6 H), 1.61 (m, 2 × CH₂, 4 H), 2.75 (s, Phen-CH₃, 3 H), 3.07 (m, 2 × NCH₂, 4 H), 5.85 (br, NH, 1 H), 5.97 (br, NH, 1 H), 6.82 (s, Phen-H₄, 1 H), 6.90-6.93 (m, Phen-H₇, Phen-H₂, 2 H), 7.17 (d, Phen-H₉, 1 H, J = 8.97 Hz), 8.14 (d, Phen-H₁, 1 H, J = 8.97 Hz), 8.24 (d, Phen-H₁₀, 1 H, J = 8.98 Hz) ppm; ¹³C-NMR (DMSO-d₆) δ: 11.9, 11.97, 23.15, 44.88, 103.08, 106.11, 115.92, 120.11, 121.79, 122.3, 123.77, 125.31, 143.5, 146.79, 147.95, 156.82 ppm; IR (KBr) ν: 3420, 3280, 2960, 2930, 2880, 1620, 1580, 1510, 1475, 1430, 1390, 1365, 1250, 1220, 1180, 1150, 1075, 1010, 950, 830, 810, 720, 670 cm⁻¹; Anal. Calcd for C₂₀H₂₅N₃ (Mr = 307.44): C 78.14, H 8.20, N 13.67 %; Found: C 78.41, H 7.98, N 13.56 %.

3,8-Bis-[3-(urac-1-yl)propyl]amino-6-methylphenantridine (2) was obtained as a red solid in 74 yield; mp 129-134 °C; ¹H-NMR (DMSO-d₆) δ: 1.96 (br, 2 × CH₂, 4 H), 2.85 (s, Phen-CH₃, 3 H), 3.18 (br, 2 × NCH₂, 4 H), 3.83 (t, 2 × CH₂Ura, 4 H, J = 6.84 Hz), 5.57 (d, 2 × Ura-H₅, 2 H, J = 7.16 Hz), 6.18 (s, 2 × NH, 2 H), 6.91 (s, Phen-H₄, 1 H), 6.99-7.02 (m, Phen-H₇, Phen-H₂, 2 H), 7.27 (d, Phen-H₉, 1 H, J = 9.03 Hz), 7.71 (d, 2 × Ura-H₆, 2 H, J = 7.78 Hz), 8.26 (d, Phen-H₁, 1 H, J = 9.03 Hz), 8.34 (d, Phen-H₁₀, 1 H, J = 9.03 Hz), 11.29 (s, 2 × Ura-NH, 2 H) ppm; IR (KBr) ν: 3350, 2920, 1660, 1610, 1570, 1505, 1450, 1340, 1330, 1280, 1230, 1170, 1150, 1050, 800, 750, 705 cm⁻¹; ES-MS (m/z) calcd: 574.3 (M⁺+ 1), 287.6 (M²⁺+ 2), 192.1 (M²⁺+ 3); found: 574.0 (M⁺+ 1), 287.7 (M²⁺+ 2), 192.2 (M²⁺+ 3).

3,8-Bis[3-(aden-9-yl)propyl]amino-6-methylphenantridine (3) was obtained as a red solid in 84 % yield; mp >300 °C; ¹H-NMR (DMSO-d₆) 2.28 (br, 2 × CH₂, 4 H), 2.84 (s, Phen-CH₃, 3 H), 3.27 (m, 2 × NCH₂, 4 H), 4.42 (br, 2 × CH₂Ade, 4 H, J = 6.84 Hz), 6.12 (br, NH, 1 H), 6.26 (br, NH, 1 H), 6.97 (s, Phen-H₄, 1 H), 7.03-7.07 (m, Phen-H₇, Phen-H₂, 2 H), 7.31 (m, Phen-H₉, NH₂, 3 H), 8.27 and 8.30 (s, 2 × Ade-H₂, 2 × Ade-H₈, 4 H), 8.43 (m, Phen-H₁, Phen-H₁₀, 2 H) ppm; IR (KBr) ν: 3300, 3100, 2910, 2840, 1650, 1600, 1570, 1505, 1460, 1405, 1380, 1330, 1300, 1240, 1190, 1155, 1000, 800, 710, 640

Supplementary Material (ESI) for Chemical Communications
This journal is © The Royal Society of Chemistry 2005

cm^{-1} ; ES-MS (m/z) calcd: 528.2 ($\text{M}^+ + 1$), 264.6 ($\text{M}^{2+} + 2$); found: 528.1 ($\text{M}^+ + 1$), 264.7 ($\text{M}^{2+} + 2$).

General Procedures

$^1\text{H-NMR}$ spectra were recorded on Varian-Gemini 300 operating at 300 MHz, as well as on Bruker Avance DRX 500 operating at 500 MHz. Chemical shifts (δ) are expressed in ppm downfield from tetramethylsilane, and J values in Hz. Signal multiplicities are denoted as s (singlet), d (doublet), t (triplet), q (quartet) and m (multiplet). The electronic absorption spectra were obtained on Varian Cary 100 Bio spectrometer. Fluorescence spectra were recorded on a Varian Cary Eclipse fluorimeter in quartz cuvettes (1 cm). IR spectra were recorded on Perkin-Elmer 297 instruments using KBr pellets. Mass spectra were obtained using Waters Micromass ZQ. The measurements were performed in aqueous buffer solution (pH = 5, sodium citrate buffer, $I=0.027 \text{ mol dm}^{-3}$). Under the experimental conditions absorbance of **1-3** were proportional to their concentrations. Polynucleotides were purchased as noted: poly A – poly U, poly dA-poly dT, poly dAdT-poly dAdT, poly A (Sigma), calf thymus (*ct*)-DNA (Aldrich). Polynucleotides were dissolved Na-cacodylate buffer, $I = 0.05 \text{ mol dm}^{-3}$, pH=7. Calf thymus (*ct*)-DNA was additionally sonicated and filtered through a $0.45 \mu\text{m}$ filter.^{2,3} Polynucleotide concentration was determined spectroscopically³ as the concentration of phosphates. Spectroscopic titrations were performed by adding portions of polynucleotide solution into the solution of the studied compound.

Under the experimental conditions used the absorbance and fluorescence intensities of **1-3** were proportional to their concentrations. Obtained data were corrected for dilution. Fluorimetric titrations were performed at pH = 5 ($I=0.027 \text{ mol dm}^{-3}$, sodium citrate/HCl buffer), $\lambda_{\text{exc}}=465 - 500 \text{ nm}$, $\lambda_{\text{em}}=530 - 650 \text{ nm}$. Processing of titration data by means of Scatchard equation gave values of ratio $n=0.1\pm 0.03$, for easier comparison all K_s values were re-calculated for fixed $n=0.1$.⁴ Values for K_s and n given in Table 2 all have satisfactory correlation coefficients (>0.99). Thermal melting curves for DNA, RNA and their complexes with studied compounds were determined as previously described³ by following the absorption change at 260 nm as a function of temperature. Absorbance of the ligands was subtracted from every curve, and the absorbance scale was normalized.

Supplementary Material (ESI) for Chemical Communications
This journal is © The Royal Society of Chemistry 2005

T_m values are the midpoints of the transition curves, determined from the maximum of the first derivative and checked graphically by the tangent method.³ ΔT_m values were calculated subtracting T_m of the free nucleic acid from T_m of the complex. Every ΔT_m value here reported was the average of at least two measurements, the error in ΔT_m is ± 0.5 °C.

Molecular modelling methods

Semiempirical calculations were performed with the program MOPAC, using AM1 calculations.

Force field calculations were performed using the all-atom AMBER force field⁵, and the partial atomic charges derived from the electrostatic potential fitted AM1 calculations. Energy minimization was performed by the steepest descent and conjugate gradients algorithms. Systems were optimized up to the convergence of about 0.01 kcal/mol. Molecular dynamic simulations were accomplished using the time step of 1 fs and the Verlet integration method. MD simulations with the explicit water molecules were performed using PBC with the cubic unit cell dimensions 31 x 31 x 31 Å. NVT assemble was used and the cutoff distances of 13 and 15 Å. System was equilibrated for 3000 steps and then the temperature was slowly increasing 50K/1000 steps up to 300K. At room temperature simulation was performed in duration of about 1 ns.

Complex of double stranded DNA, poly dA - poly dT, was build using the structure of the DNA (5'-D(CpGpApTpCpG)-3') adriamycin complex as a crude template, PDB code 154D⁶. A few different starting conformations were modeled and energy optimized. Optimized structures were subjected to MD simulation. For the DNA-DU complexes MD simulations were performed in two stages: in the first stage, during the equilibration the outside pairs of nucleotides were fixed, and the inner pairs of nucleotides were restrained to their initial position with a harmonic force of 30 kcal/mol. The restrain was gradually decreased to zero during the heating procedure. During the second stage of MD simulation, and final optimisations the surface pairs of nucleotides were restrained to their initial position with a harmonic force of 25 kcal/mol, and the inner pairs and polynucleotide were free to move.

Raw data of thermal melting experiments:

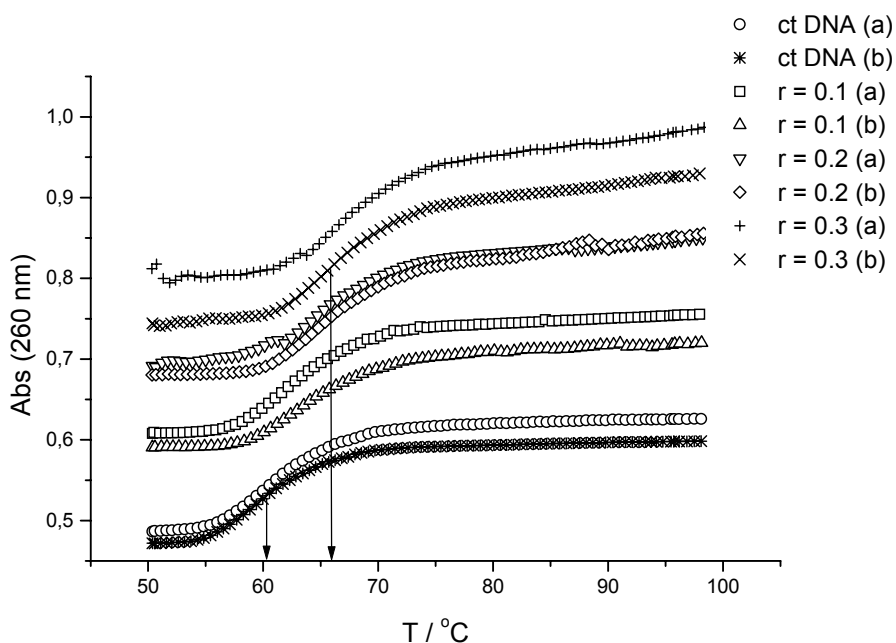


Figure 1. Melting curves of ct DNA and **1** at pH = 5.0 ((sodium citrate buffer, $I = 0.027 \text{ mol dm}^{-3}$), the $([1]/ [\text{polynucleotide phosphate}])$ ratios r are: 0.0; 0.1; 0.2; 0.3. For measuring conditions see **General Procedures**.

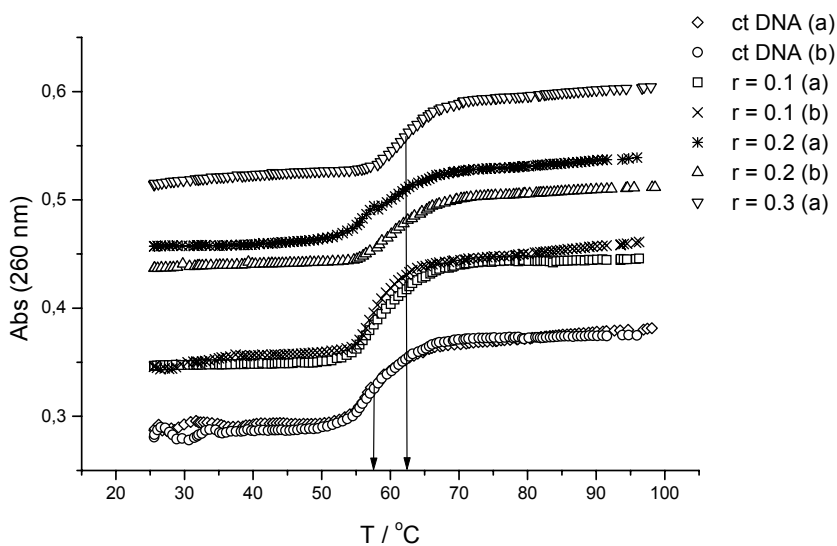


Figure 2. Melting curves of ct DNA and **2** at pH = 5.0 ((sodium citrate buffer, $I = 0.027 \text{ mol dm}^{-3}$), the $([2]/ [\text{polynucleotide phosphate}])$ ratios r are: 0.0; 0.1; 0.2; 0.3. For measuring conditions see **General Procedures**.

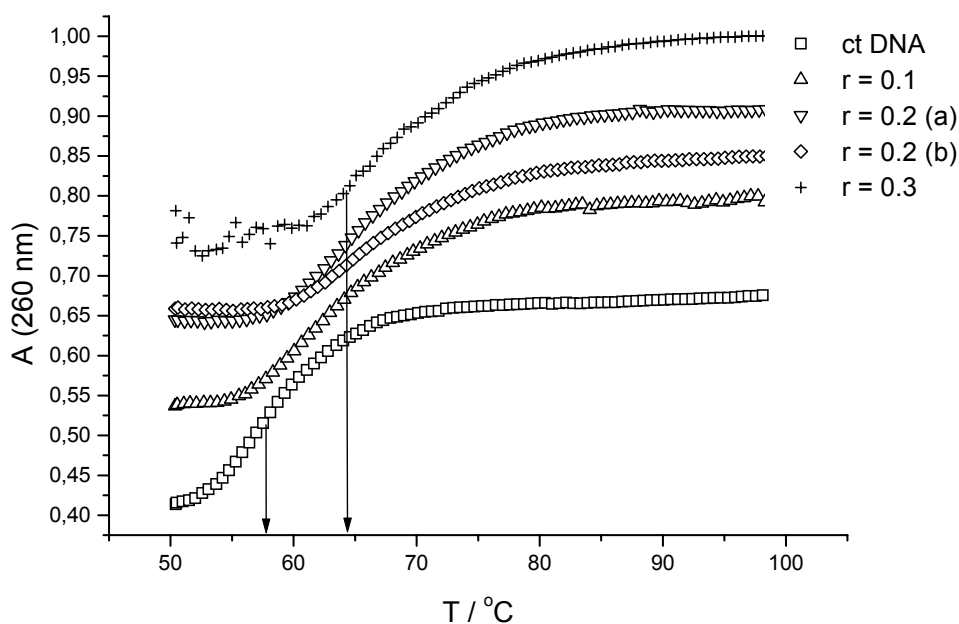


Figure 3. Melting curves of ct DNA and **3** at pH = 5.0 ((sodium citrate buffer, $I = 0.027$ mol dm⁻³), the $([3]/ [\text{polynucleotide phosphate}])$ ratios r are: 0.0; 0.1; 0.2; 0.3. For measuring conditions see General Procedures.

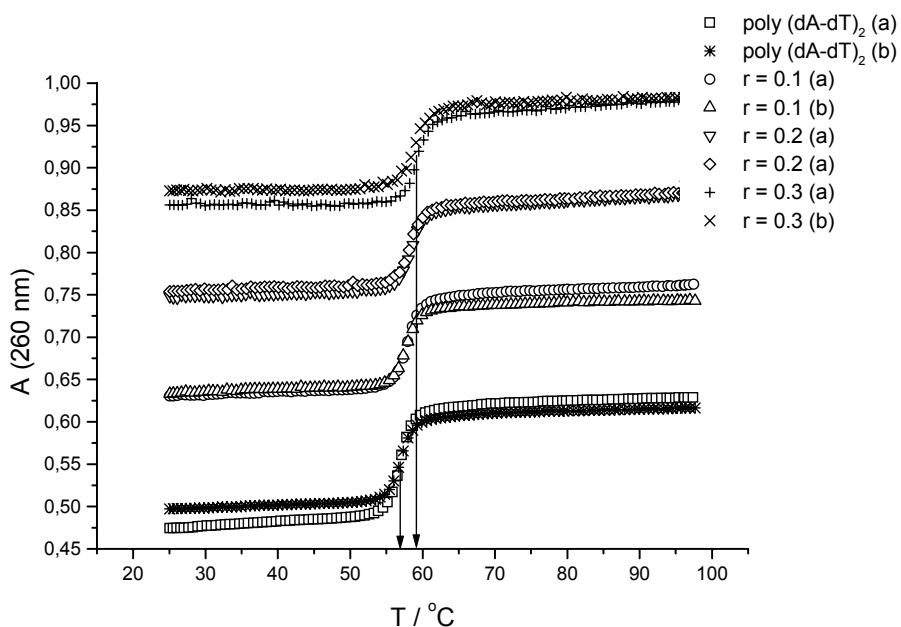


Figure 4. Melting curves of poly (dA-dT)₂ and **1** at pH = 5.0 ((sodium citrate buffer, $I = 0.027$ mol dm⁻³), the $([1]/ [\text{polynucleotide phosphate}])$ ratios r are: 0.0; 0.1; 0.2; 0.3. For measuring conditions see General Procedures.

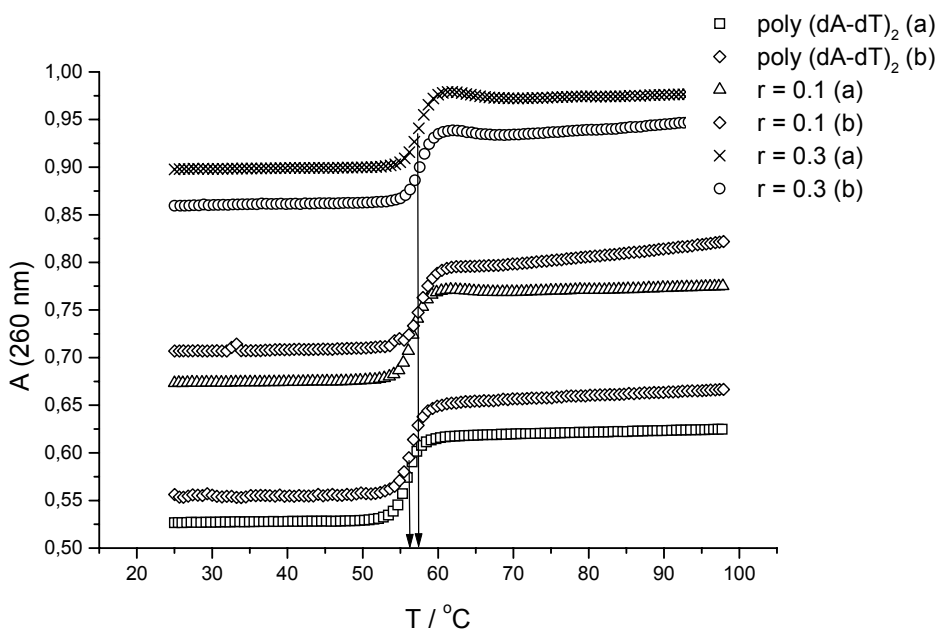


Figure 5. Melting curves of poly (dA-dT)₂ and **2** at pH = 5.0 ((sodium citrate buffer, $I = 0.027 \text{ mol dm}^{-3}$), the ($[2]/$ [polynucleotide phosphate]) ratios r are: 0.0; 0.1; 0.3. For measuring conditions see General Procedures.

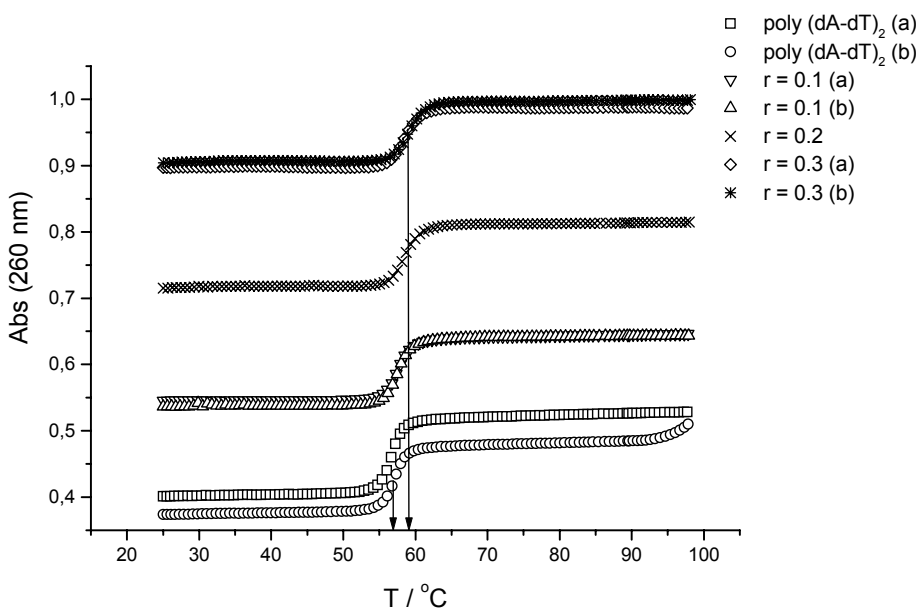


Figure 6. Melting curves of poly (dA-dT)₂ and **3** at pH = 5.0 ((sodium citrate buffer, $I = 0.027 \text{ mol dm}^{-3}$), the ($[3]/$ [polynucleotide phosphate]) ratios r are: 0.0; 0.1; 0.2; 0.3. For measuring conditions see General Procedures.

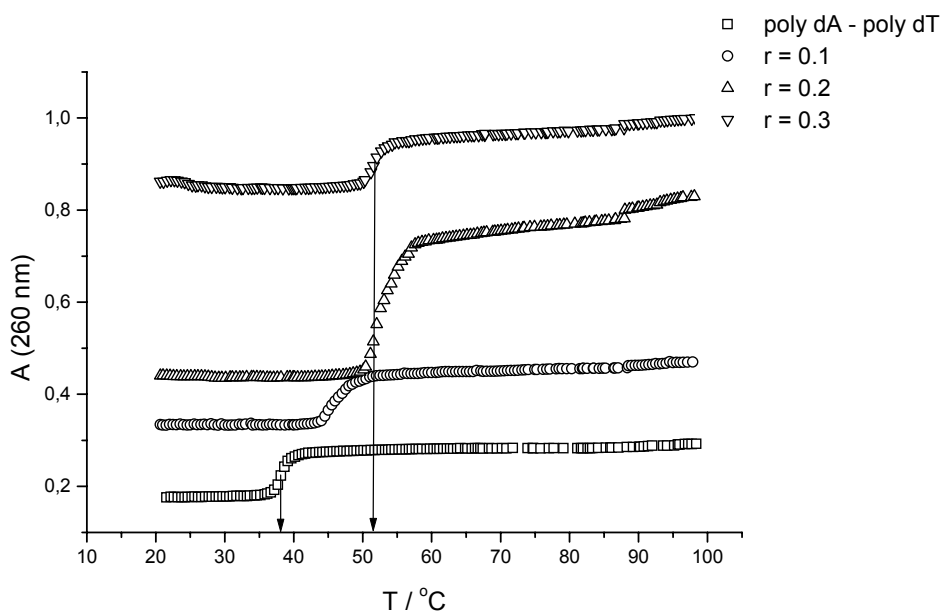


Figure 7. Melting curves of poly dA-poly dT and **1** at pH = 5.0 ((sodium citrate buffer, $I = 0.027 \text{ mol dm}^{-3}$), the ($[1]/ [\text{polynucleotide phosphate}]$) ratios r are: 0.0; 0.1; 0.2; 0.3. For measuring conditions see General Procedures.

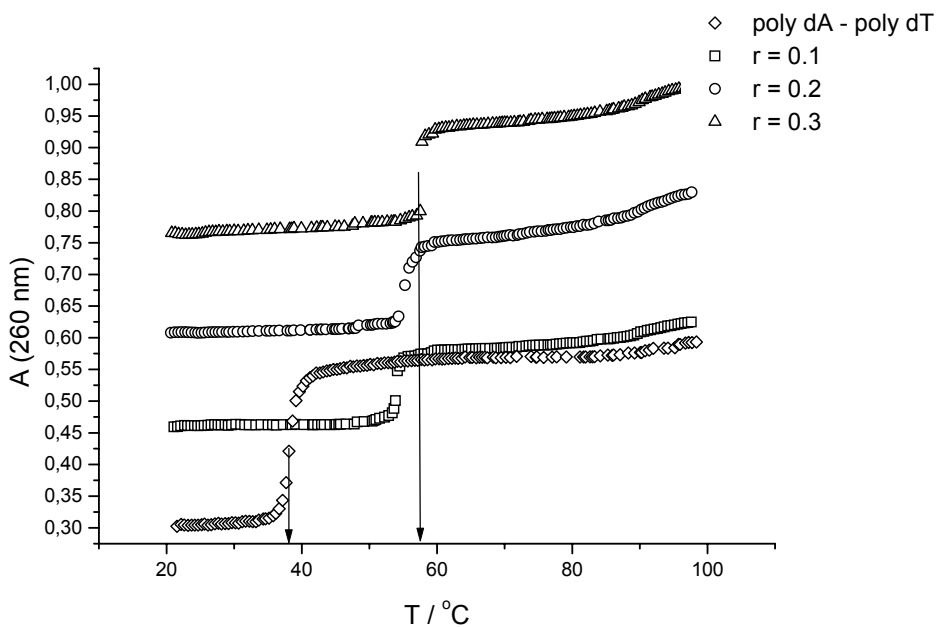


Figure 8. Melting curves of poly dA-poly dT and **2** at pH = 5.0 ((sodium citrate buffer, $I = 0.027 \text{ mol dm}^{-3}$), the ($[2]/ [\text{polynucleotide phosphate}]$) ratios r are: 0.0; 0.1; 0.2; 0.3. For measuring conditions see General Procedures.

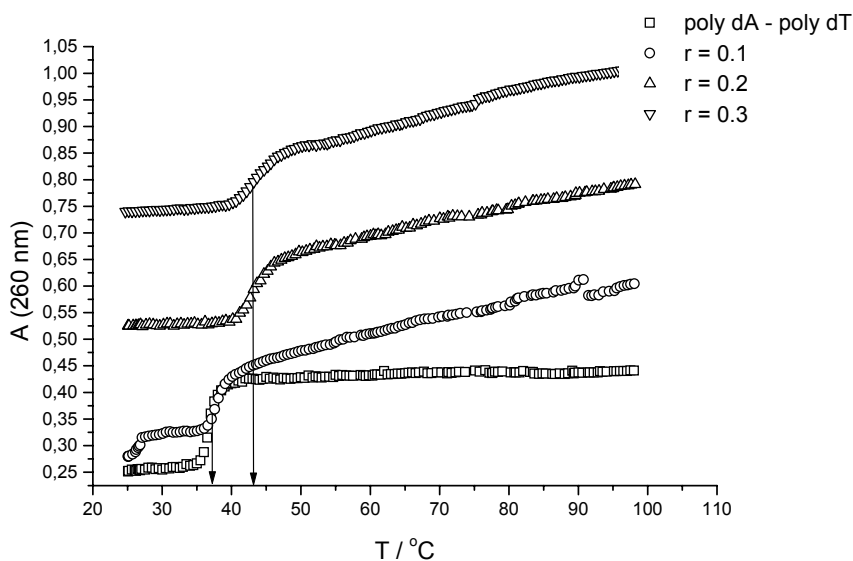


Figure 9. Melting curves of poly dA-poly dT and **3** at pH = 5.0 ((sodium citrate buffer, $I = 0.027 \text{ mol dm}^{-3}$), the ($[3]/ [\text{polynucleotide phosphate}]$) ratios r are: 0.0; 0.1; 0.2; 0.3. For measuring conditions see General Procedures.

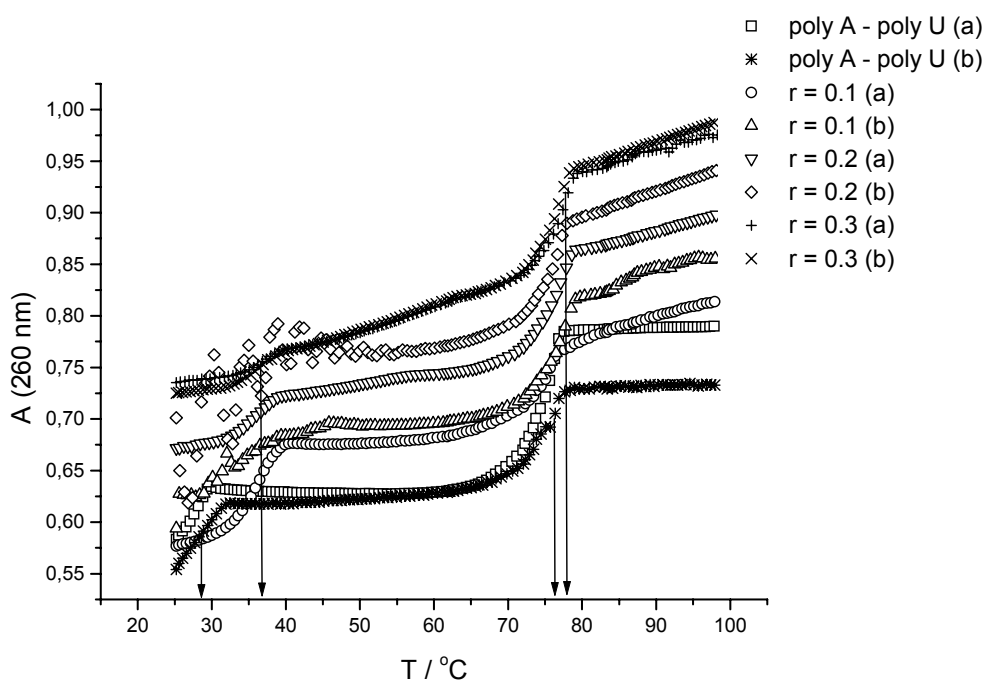


figure 10. Melting curves of poly A-poly U and **1** at pH = 5.0 ((sodium citrate buffer, $I = 0.027 \text{ mol dm}^{-3}$), the ($[1]/ [\text{polynucleotide phosphate}]$) ratios r are: 0.0; 0.1; 0.2; 0.3. For measuring conditions see General Procedures.

F

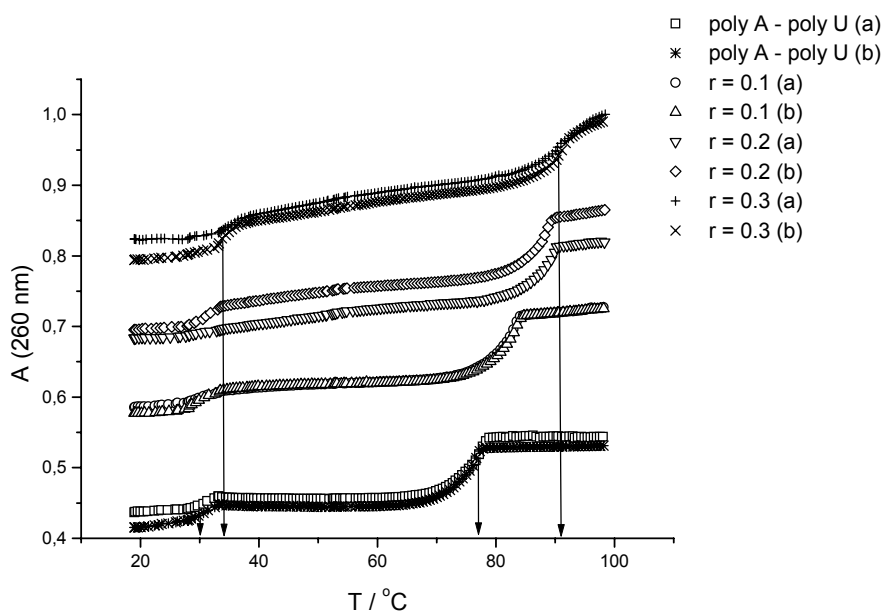


Figure 11. Melting curves of poly A-poly U and **2** at pH = 5.0 ((sodium citrate buffer, $I = 0.027 \text{ mol dm}^{-3}$), the ($[2]/[\text{polynucleotide phosphate}]$) ratios r are: 0.0; 0.1; 0.2; 0.3. For measuring conditions see General Procedures.

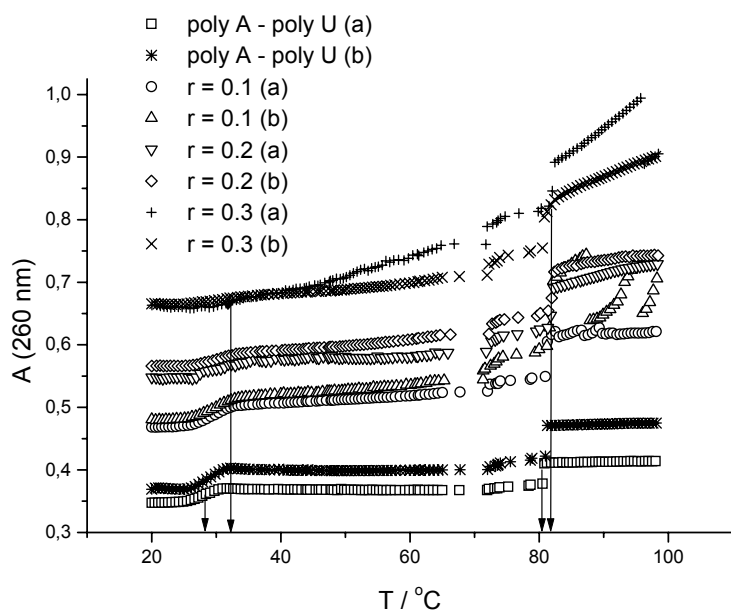


Figure 12. Melting curves of poly A-poly U and **3** at pH = 5.0 ((sodium citrate buffer, $I = 0.027 \text{ mol dm}^{-3}$), the ($[3]/[\text{polynucleotide phosphate}]$) ratios r are: 0.0; 0.1; 0.2; 0.3. For measuring conditions see General Procedures.

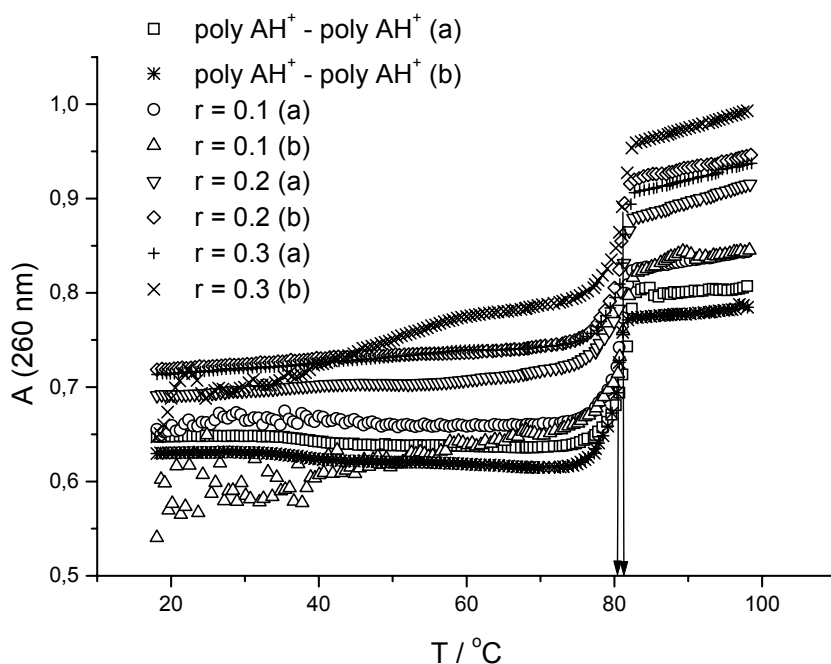


Figure 13. Melting curves of poly A-poly U and **1** at pH = 5.0 ((sodium citrate buffer, $I = 0.027 \text{ mol dm}^{-3}$), the ($[1]/ [\text{polynucleotide phosphate}]$) ratios r are: 0.0; 0.1; 0.2; 0.3. For measuring conditions see General Procedures.

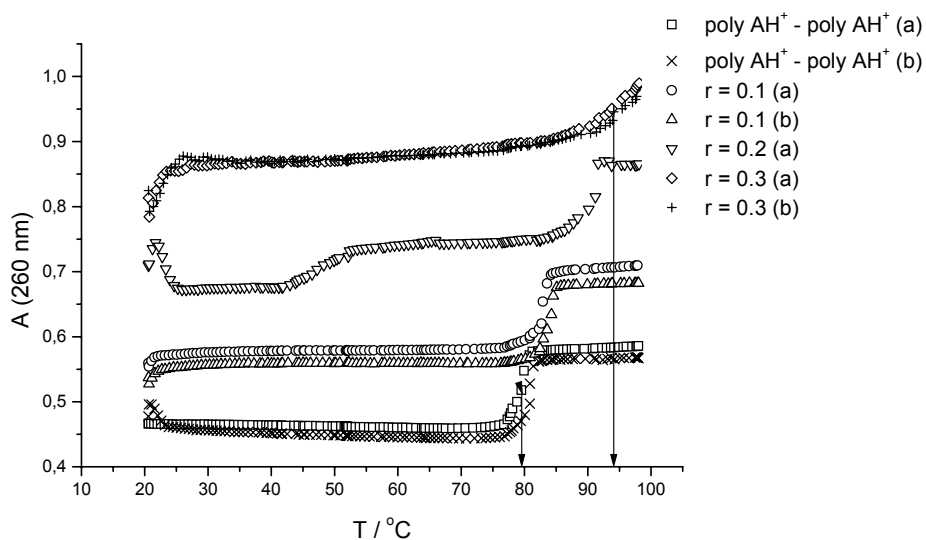


Figure 14. Melting curves of poly A-poly U and **2** at pH = 5.0 ((sodium citrate buffer, $I = 0.027 \text{ mol dm}^{-3}$), the ($[2]/ [\text{polynucleotide phosphate}]$) ratios r are: 0.0; 0.1; 0.2; 0.3. For measuring conditions see General Procedures.

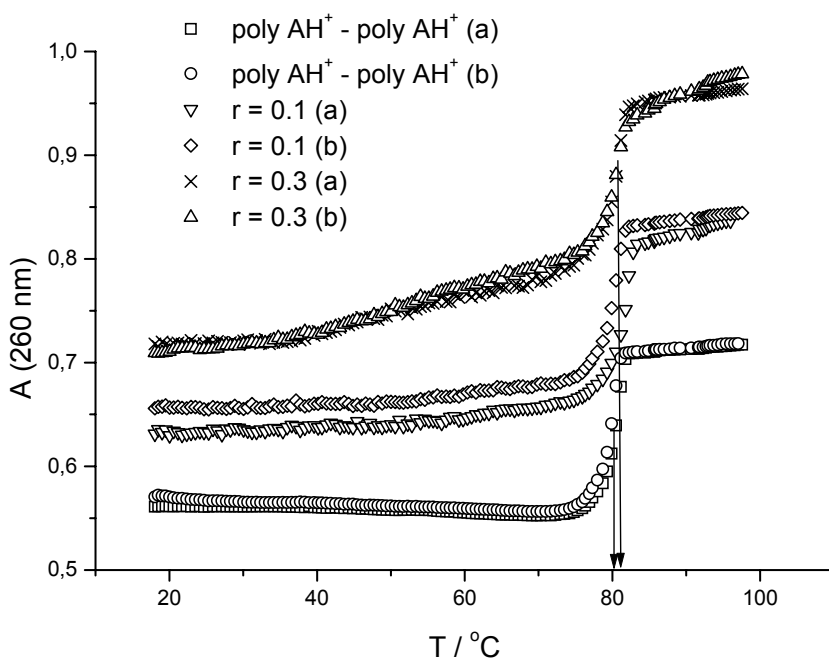


Figure 15. Melting curves of poly A-poly U and **3** at pH = 5.0 ((sodium citrate buffer, $I = 0.027 \text{ mol dm}^{-3}$), the ($[3]/ [\text{polynucleotide phosphate}]$) ratios r are: 0.0; 0.1; 0.3. For measuring conditions see General Procedures.

Fluorescence measurements

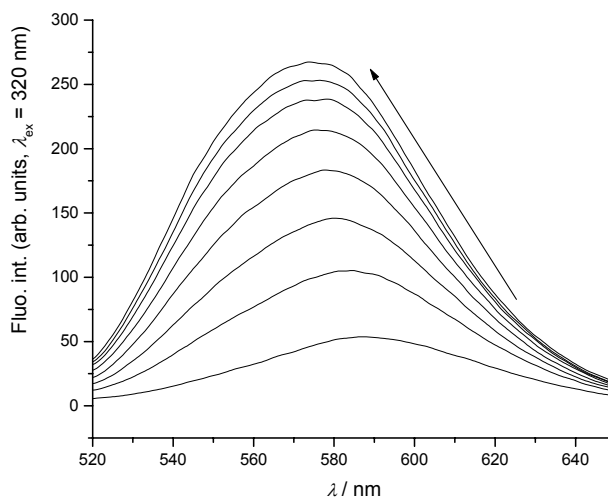


Figure 16. Fluorimetric titration of **1**, $c = 4.8 \times 10^{-6} \text{ mol dm}^{-3}$ with ct DNA (pH = 5, sodium citrate buffer, $I = 0.027 \text{ mol dm}^{-3}$, $c(\text{ct DNA}) = 7.98 \times 10^{-6} \text{ mol dm}^{-3} - 1.98 \times 10^{-4} \text{ mol dm}^{-3}$). For measuring conditions see General Procedures.

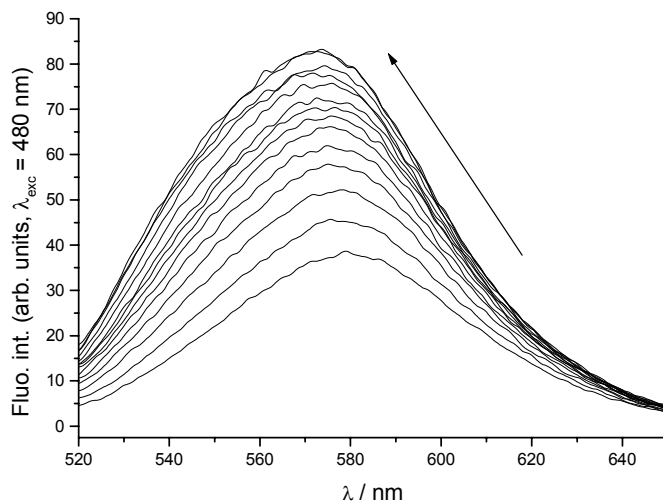


Figure 17. Fluorimetric titration of **2**, $c = 2.4 \times 10^{-6} \text{ mol dm}^{-3}$ with ct DNA (pH = 5, sodium citrate buffer, $I=0.027 \text{ mol dm}^{-3}$, $c(\text{ct DNA}) = 1.08 \times 10^{-5} \text{ mol dm}^{-3} - 8.08 \times 10^{-4} \text{ mol dm}^{-3}$). For measuring conditions see General Procedures.

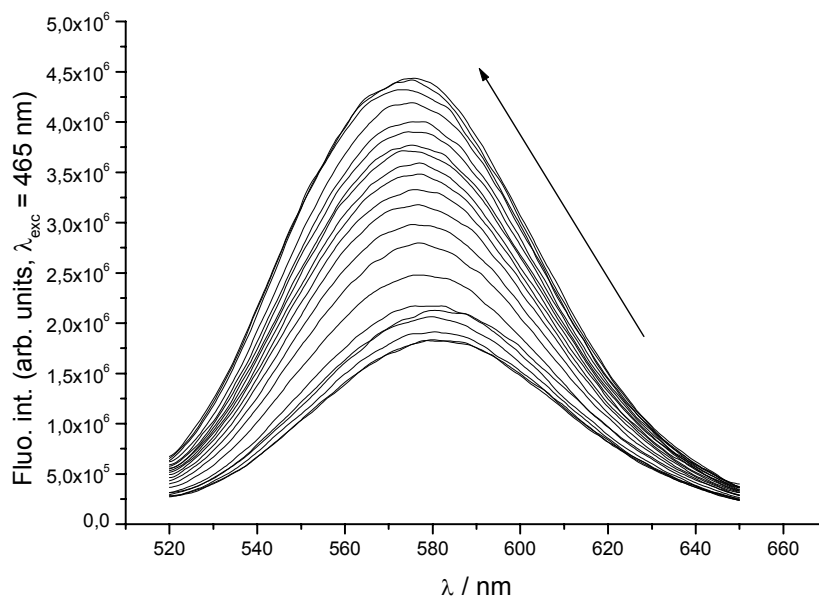


Figure 18. Fluorimetric titration of **3**, $c = 5.0 \times 10^{-6} \text{ mol dm}^{-3}$ with ct DNA (pH = 5, sodium citrate buffer, $I=0.027 \text{ mol dm}^{-3}$, $c(\text{ct DNA}) = 3.2 \times 10^{-6} \text{ mol dm}^{-3} - 5.52 \times 10^{-4} \text{ mol dm}^{-3}$). For measuring conditions see General Procedures.

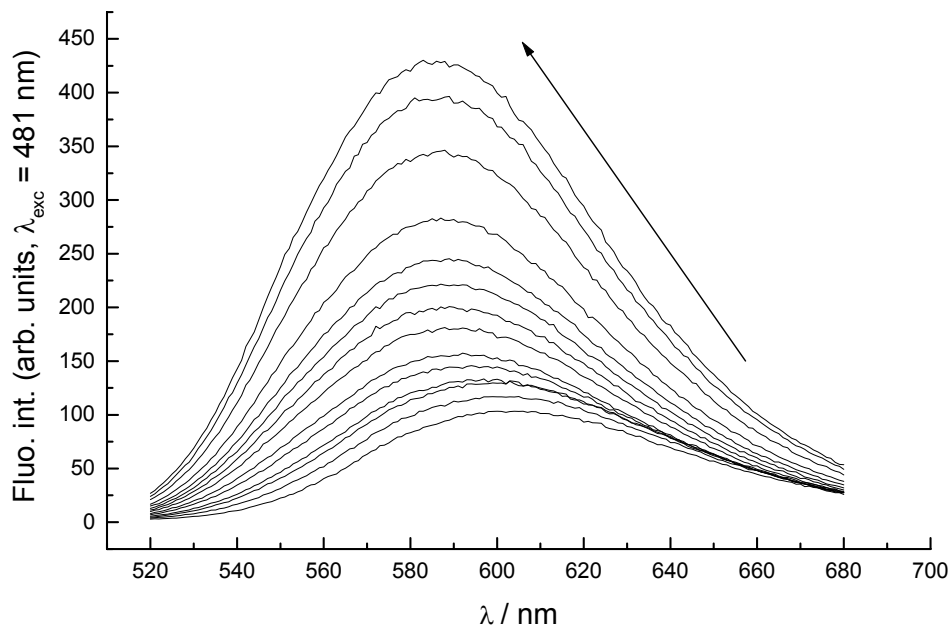


Figure 19. Fluorimetric titration of **1**, $c = 2,14 \times 10^{-6} \text{ mol dm}^{-3}$ with poly dAdT – poly dAdT (pH = 5, sodium citrate buffer, $I=0.027 \text{ mol dm}^{-3}$, $c (\text{poly dAdT – poly dAdT}) = 3.84 \times 10^{-6} \text{ mol dm}^{-3} - 3.81 \times 10^{-4} \text{ mol dm}^{-3}$. For measuring conditions see General Procedures.

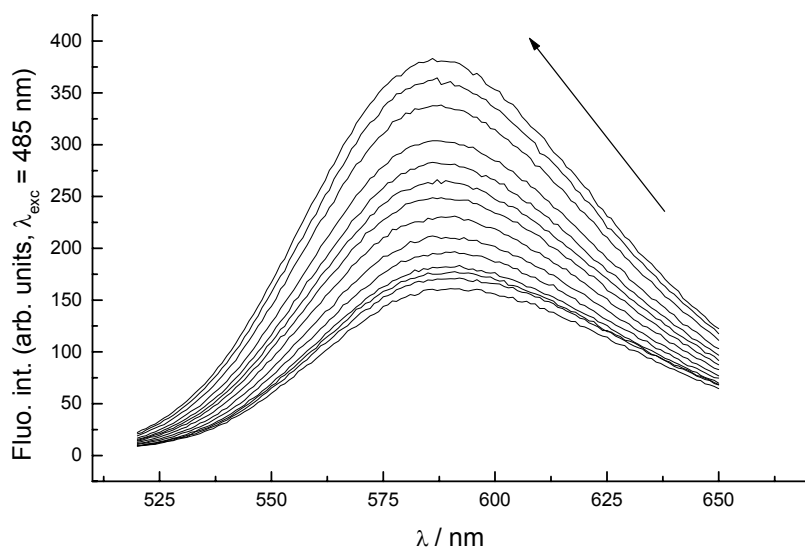


Figure 20. Fluorimetric titration of **2**, $c = 2.15 \times 10^{-6} \text{ mol dm}^{-3}$ with poly dAdT – poly dAdT (pH = 5, sodium citrate buffer, $I=0.027 \text{ mol dm}^{-3}$, $c (\text{poly dAdT – poly dAdT}) = 3.14 \times 10^{-6} \text{ mol dm}^{-3} - 3.53 \times 10^{-4} \text{ mol dm}^{-3}$. For measuring conditions see General Procedures.

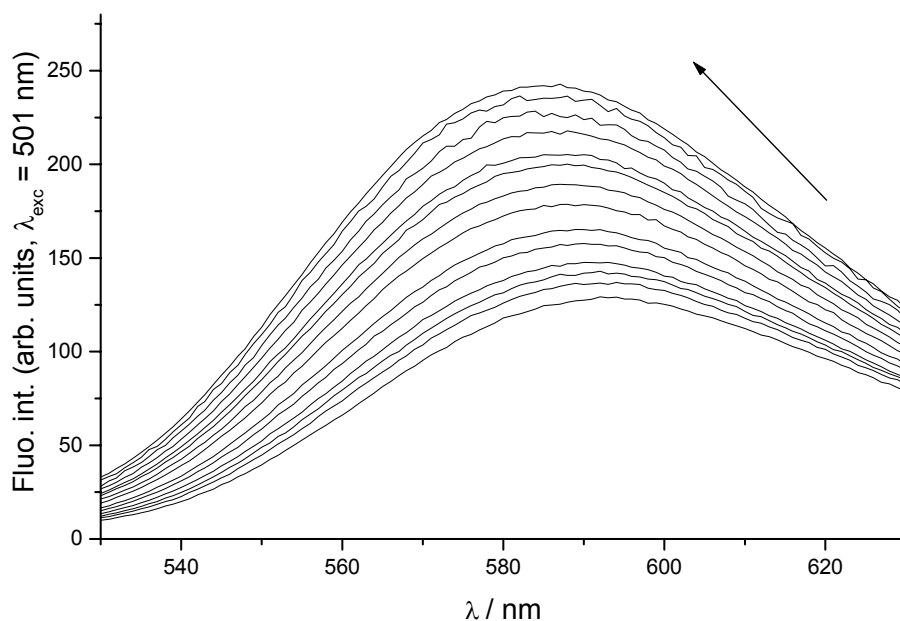


Figure 21. Fluorimetric titration of **3**, $c = 2.12 \times 10^{-6} \text{ mol dm}^{-3}$ with poly dAdT – poly dAdT (pH = 5, sodium citrate buffer, $I=0.027 \text{ mol dm}^{-3}$, $c(\text{poly dAdT} - \text{poly dAdT}) = 3.0 \times 10^{-6} \text{ mol dm}^{-3} - 3.0 \times 10^{-4} \text{ mol dm}^{-3}$). For measuring conditions see General Procedures.

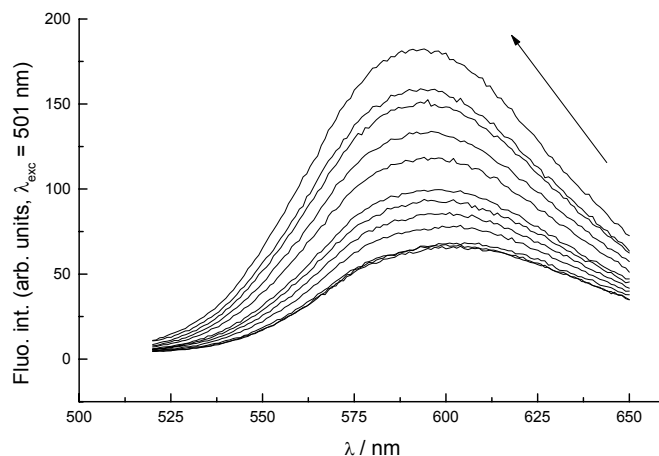


Figure 22. Fluorimetric titration of **1**, $c = 2.14 \times 10^{-6} \text{ mol dm}^{-3}$ with poly dA – poly dT (pH = 5, sodium citrate buffer, $I=0.027 \text{ mol dm}^{-3}$, $c(\text{poly dA} - \text{poly dT}) = 1.45 \times 10^{-5} \text{ mol dm}^{-3} - 6.99 \times 10^{-4} \text{ mol dm}^{-3}$). For measuring conditions see General Procedures.

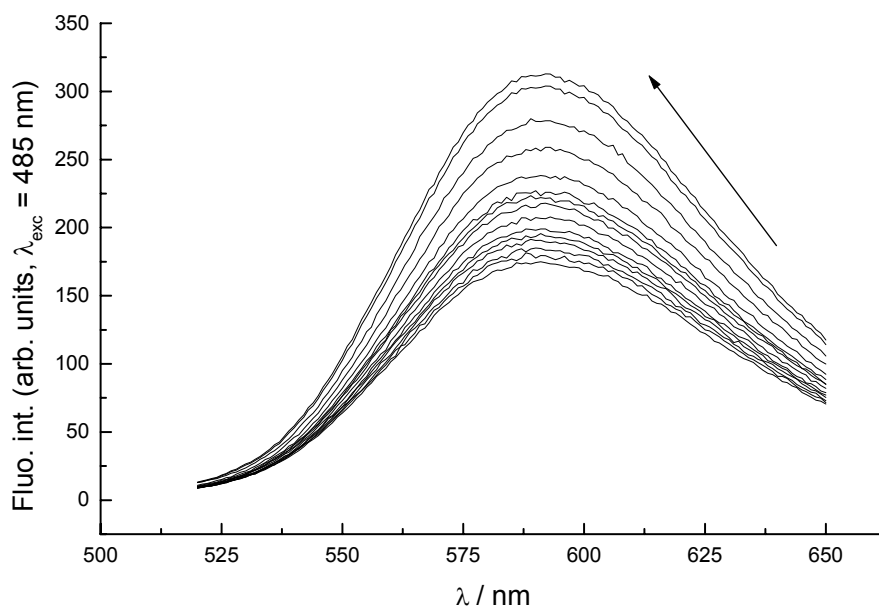


Figure 23. Fluorimetric titration of **2**, $c = 2.15 \times 10^{-6} \text{ mol dm}^{-3}$ with poly dA – poly dT (pH = 5, sodium citrate buffer, $I=0.027 \text{ mol dm}^{-3}$, $c(\text{poly dA} - \text{poly dT}) = 2.72 \times 10^{-6} \text{ mol dm}^{-3} - 3.28 \times 10^{-4} \text{ mol dm}^{-3}$. For measuring conditions see General Procedures.

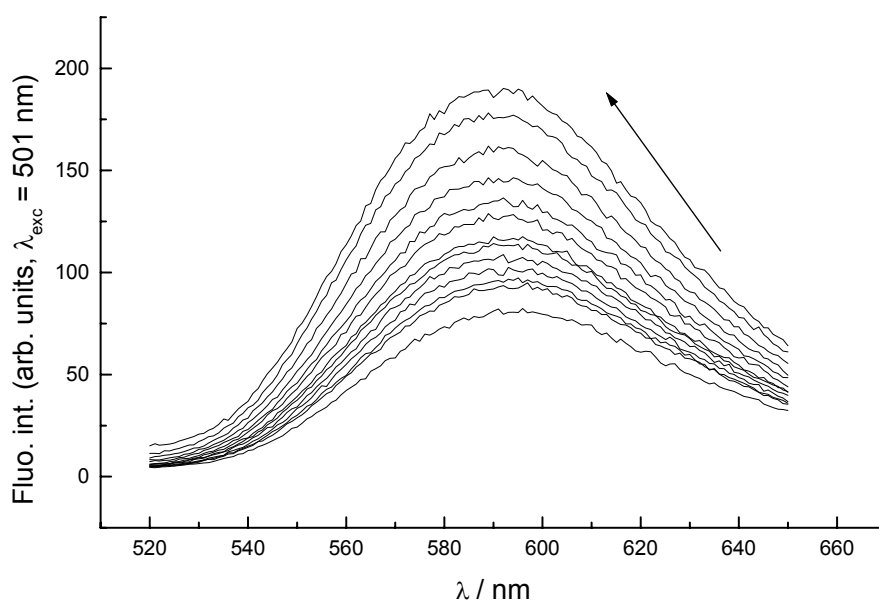


Figure 24. Fluorimetric titration of **3**, $c = 2.12 \times 10^{-6} \text{ mol dm}^{-3}$ with poly dA – poly dT (pH = 5, sodium citrate buffer, $I=0.027 \text{ mol dm}^{-3}$, $c(\text{poly dA} - \text{poly dT}) = 4.07 \times 10^{-6} \text{ mol dm}^{-3} - 3.17 \times 10^{-4} \text{ mol dm}^{-3}$. For measuring conditions see General Procedures.

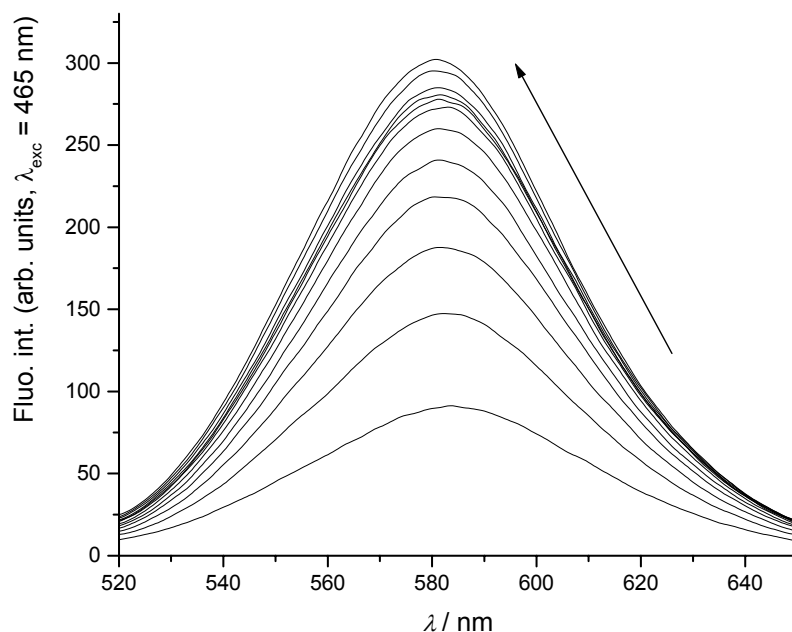


Figure 25. Fluorimetric titration of **1**, $c = 4.8 \times 10^{-6} \text{ mol dm}^{-3}$ with poly A-poly U (pH = 5, sodium citrate buffer, $I=0.027 \text{ mol dm}^{-3}$, $c(\text{poly A-poly U}) = 1.23 \times 10^{-5} \text{ mol dm}^{-3} - 1.52 \times 10^{-4} \text{ mol dm}^{-3}$. For measuring conditions see General Procedures.

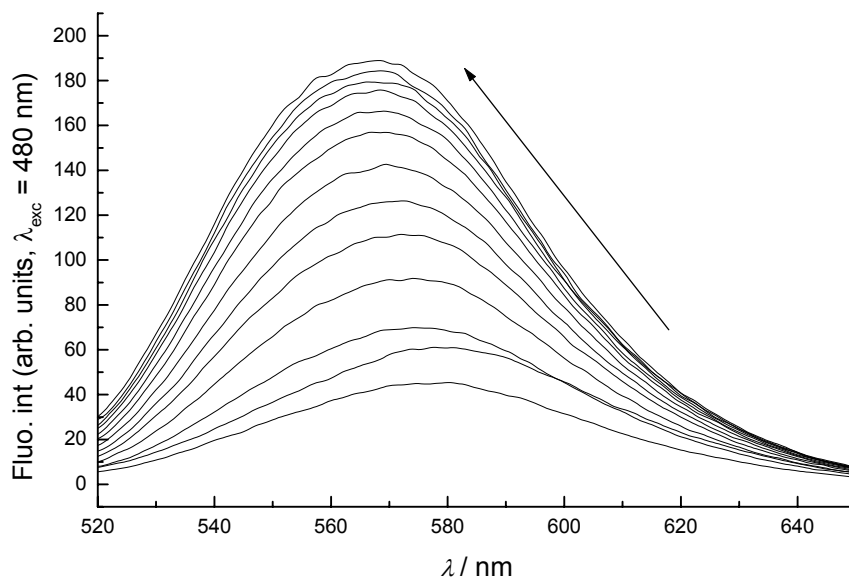


Figure 26. Fluorimetric titration of **2**, $c = 2.4 \times 10^{-6} \text{ mol dm}^{-3}$ with poly A-poly U (pH = 5, sodium citrate buffer, $I=0.027 \text{ mol dm}^{-3}$, $c(\text{poly A-poly U}) = 3.19 \times 10^{-5} \text{ mol dm}^{-3} - 9.62 \times 10^{-4} \text{ mol dm}^{-3}$. For measuring conditions see General Procedures.

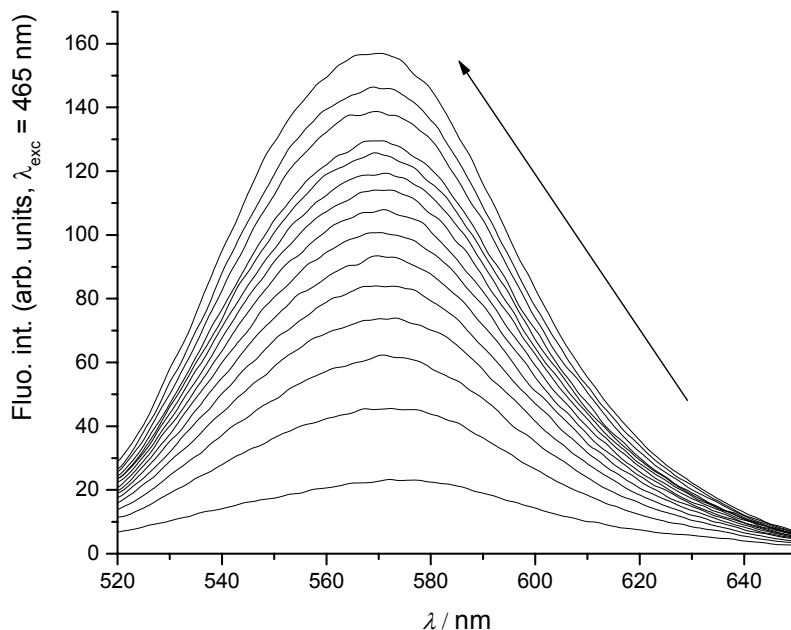


Figure 27. Fluorimetric titration of **3**, $c = 6.38 \times 10^{-6} \text{ mol dm}^{-3}$ with poly A-poly U (pH = 5, sodium citrate buffer, $I=0.027 \text{ mol dm}^{-3}$, $c(\text{poly A-poly U}) = 1.23 \times 10^{-5} \text{ mol dm}^{-3} - 2.66 \times 10^{-4} \text{ mol dm}^{-3}$). For measuring conditions see General Procedures.

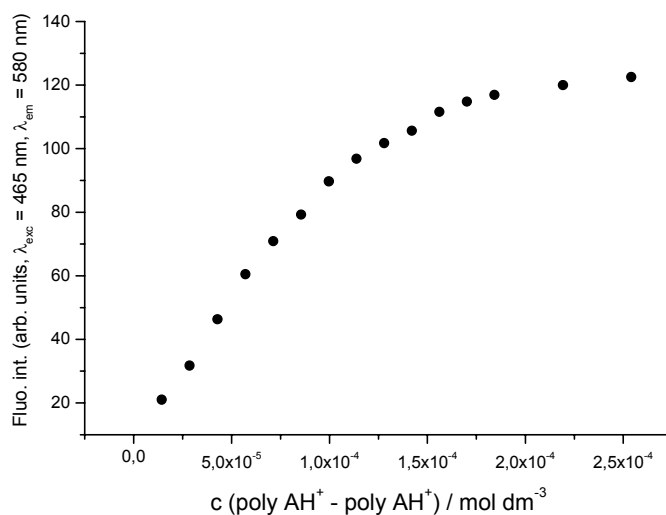


Figure 28. Fluorimetric titration (measured on single wavelength) of **1**, $c = 4.8 \times 10^{-6} \text{ mol dm}^{-3}$ with poly AH⁺ - poly AH⁺ (pH = 5, sodium citrate buffer, $I=0.027 \text{ mol dm}^{-3}$, $c(\text{poly AH}^+ - \text{poly AH}^+) = 1.43 \times 10^{-5} \text{ mol dm}^{-3} - 2.54 \times 10^{-4} \text{ mol dm}^{-3}$). For measuring conditions see General Procedures.

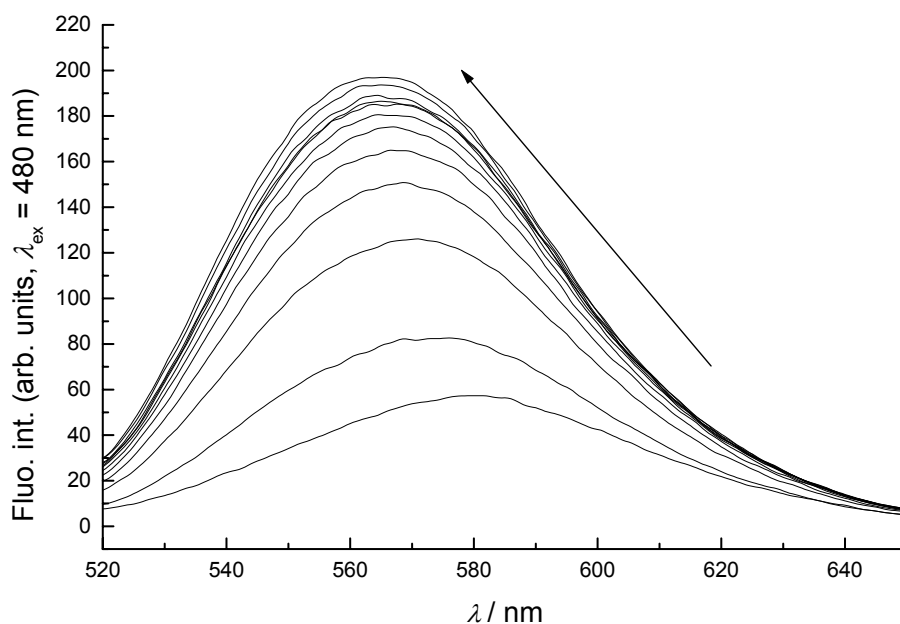


Figure 29. Fluorimetric titration of **2**, $c = 2.4 \times 10^{-6} \text{ mol dm}^{-3}$ with poly AH^+ - poly AH^+ (pH = 5, sodium citrate buffer, $I=0.027 \text{ mol dm}^{-3}$, $c(\text{poly AH}^+ - \text{poly AH}^+) = 4.23 \times 10^{-5} \text{ mol dm}^{-3} - 5.37 \times 10^{-4} \text{ mol dm}^{-3}$. For measuring conditions see General Procedures.

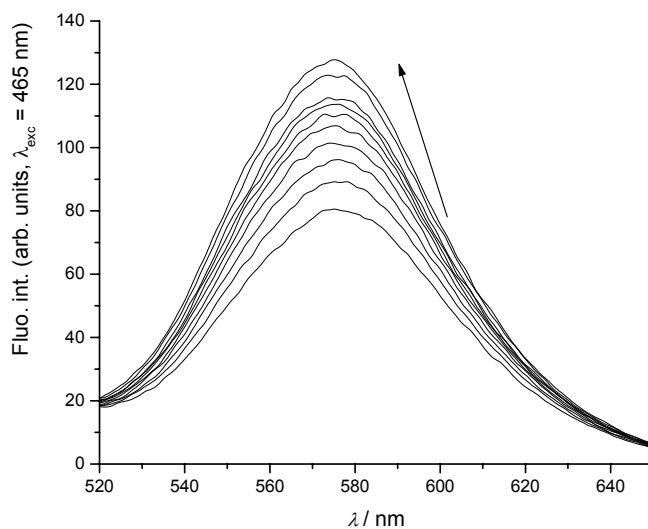


Figure 30. Fluorimetric titration of **3**, $c = 6.3 \times 10^{-6} \text{ mol dm}^{-3}$ with poly AH^+ - poly AH^+ (pH = 5, sodium citrate buffer, $I=0.027 \text{ mol dm}^{-3}$, $c(\text{poly AH}^+ - \text{poly AH}^+) = 1.43 \times 10^{-5} \text{ mol dm}^{-3} - 2.89 \times 10^{-4} \text{ mol dm}^{-3}$. For measuring conditions see General Procedures.

Supplementary Material (ESI) for Chemical Communications
This journal is © The Royal Society of Chemistry 2005

¹ L.-M. Tumor, I. Piantanida, P. Novak, M. Žinić, *J. Phys. Org. Chem.*, 2002, **15**, 599-607

² J.B. Chaires, N. Dattagupta, D.M. Crothers, *Biochemistry*, 1982, **21**, 3933-3940.

³ B.S. Palm, I. Piantanida, M. Žinić, H.-J. Schneider, *J. Chem. Soc., Perkin Trans. 2*, 2000, 385-392.

⁴ J.D. McGhee, P.H. von Hippel, *J. Mol. Biol.* 1974, **86**, 469-489.

⁵ W.D. Cornell, P. Cieplak, C.I. Payly, I.R. Gould, K.M. Merz, D.M. Ferguson, D.C. Spellmeyer, T. Fox, J.W. Caldwell, and P.A. Kollman, *J. Am. Chem. Soc.*, 1995, **117**, 5179-5197.

⁶ L.A. Lipscomb, M.E. Peek, F.X. Zhou, J.A. Bertrand, D. VanDerveer, L.D. Williams, *Biochemistry*, 1994, **33**, 3649-3659.